

Generalized Plasma Skimming Model for Cells and Drug Carriers in the Microvasculature

Tae-Rin Lee · Sung Sic Yoo · Jiho Yang

Received: date / Accepted: date

Abstract In microvascular transport, where both blood and drug carriers are involved, plasma skimming has a key role on changing hematocrit level and drug carrier concentration in capillary beds after continuous vessel bifurcation in the microvasculature. While there have been numerous studies on modeling the plasma skimming of blood, previous works lacked in consideration of its interaction with drug carriers. In this paper, a generalized plasma skimming model is suggested to predict the redistributions of both the cells and drug carriers at each bifurcation. In order to examine its applicability, this new model was applied on a single bifurcation system to predict the redistribution of red blood cells and drug carriers. Furthermore, this model was tested at microvascular network level under different plasma skimming conditions for predicting the concentration of drug carriers. Based on these results, the applicability of this generalized plasma skimming model is fully discussed and future works along with the model's limitations are summarized.

Keywords Plasma skimming · Microvascular transport · Drug carrier · Nanomedicine

1 Introduction

Drug carriers with chemotherapeutic agents are administered to macrocirculatory systems for efficient diagnosis and treatment of various diseases (Jain and Stylianopoulos

2010; Peer et al. 2007). In order to deliver drug carriers in diseased areas, the geometric difference between normal and diseased areas of microvasculatures is mainly considered (Chauhan et al. 2012). For this reason, good understanding of the physics of drug carriers in the microvasculature holds significant importance. Related to this topic, several experiments were performed to quantify the drug carrier distributions *in vitro* (Saadatmand et al. 2011; Tan et al. 2016) and *in vivo* (Chauhan et al. 2012; Kamoun et al. 2010; van de Ven et al. 2012). Even though these experimental works suggested good methods at single vessel and single bifurcation level, quantitative measurement of the drug carrier concentration in the entire microvasculature still remains as a challenge.

An alternative way of predicting the drug carrier distribution is to develop a mathematical model that can estimate the targeting efficiency of drug carriers in the microvasculature. Several computational methods were suggested and conducted to simulate various interactions between cells and drug carriers (Lee et al. 2013, 2014; Müller et al. 2014; Tan et al. 2016). Although the blood flow simulations with drug carriers in a microvessel are possible, Computational Fluid Dynamics (CFD) simulation of cells and drug carriers *in the entire microvasculature* has not been reported yet due to its tremendous efforts for a test-run. Meanwhile, mathematical models have been utilized to simplify the blood flow in microvessels by applying Poiseuille's law with the *in vivo* viscosity law (Pries et al. 1996) to calculate the blood flow in microvessels, along with conservation of mass for flow division at each bifurcation. By using these mathematical models, drug carrier distributions in the tumor microvasculature were computed at microvascular-network level (Frieboes et al. 2013; Curtis et al. 2015).

Tae-Rin Lee (✉) · Sung Sic Yoo · Jiho Yang
Advanced Institutes of Convergence Technology, Seoul National University, Suwon 443-270, Republic of Korea
e-mail: taerinlee@snu.ac.kr

Jiho Yang
Department of Computer Science, Technische Universität München, Boltzmannstraße 3, Garching, Germany

Previous mathematical models were focused on the plasma skimming (Krogh et al. 1922; Pries et al. 1996) of blood flow at each bifurcation. In the microvascular transport, red blood cells (RBCs) are concentrated on the vessel core with cell-free layer (CFL) near the vessel wall. Due to these two areas, hematocrit level is changed in following daughter vessels. The subsequent bifurcating processes change the total distribution of RBCs and blood flow characteristics in the entire microvasculature, and this is called the plasma skimming effect. However, the drug carrier distribution in the microvasculature is highly dependent on the plasma skimming of blood flow. Hence, it is important to develop a mathematical model that can predict plasma skimming effects of both blood and drug carriers considering their interactions.

Previous studies showed that their interactions depend on numerous factors including drug carriers' size, shape, and even vessel geometry (Tan et al. 2013). Both numerical simulations and experiments indicated clear interactions between drug carriers and RBCs (Müller et al. 2014; D'Apolito et al. 2016). Lee et al. studied that the cross-sectional distribution of drug carriers depend on their size, and that larger particles tend to marginate towards vessel walls (Lee et al. 2013). On the other hand, Muro et al. and also Namdee et al. observed that larger particles can result in lower targeting efficiency (Muro et al. 2008; Namdee et al. 2014). These findings highlight that whilst drug carriers and RBCs clearly interact with great significance, there is no absolute rule to describe how they interact and how drug carriers distribute (Champion et al. 2008; Sobczynski et al. 2015). Therefore, it is necessary to study the drug carrier distribution and its delivery by coupling it with plasma skimming and the resulting interactions. Moreover, this must be conducted in a generalized fashion and also in simplest form for computationally efficient prediction. In this paper, a generalized plasma skimming model for cells and drug carriers in the microvas-

culature is suggested. To achieve this goal, the recently developed plasma skimming model for blood in micro-circulatory networks (Gould and Linninger 2015) is applied, and extended to the scope of both cells and drug carriers. Two cases with different drug carrier distribution condition in a single bifurcation model are considered to validate the model. Furthermore, the generalized plasma skimming model is tested at microvascular network level for estimating distributions of cells and drug carriers. In addition, the limitation of current mathematical model and future perspectives are briefly discussed.

2 Materials and Methods

2.1 Plasma skimming model for blood

In a parent vessel, blood flow is determined by blood viscosity, hematocrit, vessel geometry, and pressure drop. After bifurcation, the blood flow characteristics in the following daughter vessels are changed due to their diameter reduction. The flow rate in the daughter vessel can be easily calculated by using conservation of mass with the diameters of daughter vessels. In the parent vessel, RBCs are concentrated on the core of microvessel with a certain thickness of CFL. Then, the thinner daughter vessel, as a side branch, takes less RBCs and more plasma. On the other hand, the thicker daughter vessel takes more RBCs and less plasma. As shown in Fig. 1, the thicker daughter vessel has higher hematocrit (hemoconcentration) than the parent vessel and the thinner vessel has lower hematocrit (hemodilution). This phenomenon is called the "plasma skimming". To model the plasma skimming parametrically, Gould and Linninger (2015) suggested a drift parameter, M . The general steps to determine hematocrit changes in a bifurcation are as follows:

$$H_1 = H_0 - \Delta H = \zeta_1^b H^* \quad (1)$$

$$H_2 = \zeta_2^b H^* \quad (2)$$

$$Q_0 H_0 = Q_1 H_1 + Q_2 H_2 = Q_1 \zeta_1^b H^* + Q_2 \zeta_2^b H^* \quad (3)$$

$$\zeta_i^b = \left(\frac{A_i}{A_0} \right)^{\frac{1}{M}} \quad \text{where } i = 1, 2 \quad (4)$$

where H is the hematocrit, ζ^b is the hematocrit change coefficient due to plasma skimming, Q is the flow rate, A is the cross-sectional area of each vessel, and subscript 0, 1 and 2 indicate the parent, and two daughter

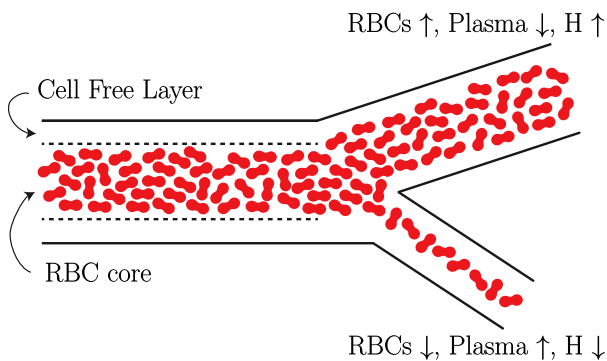


Fig. 1 Plasma skimming of RBCs at a bifurcation.

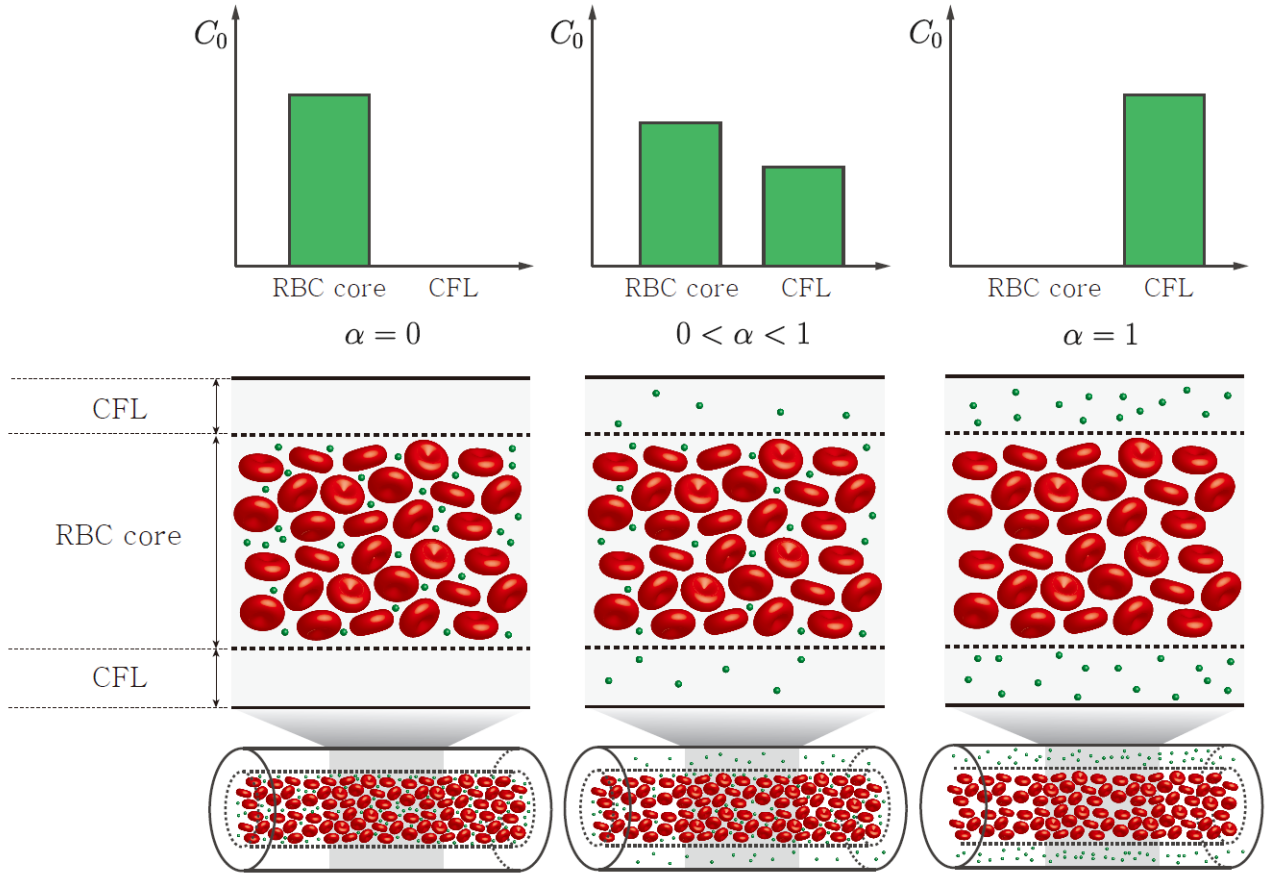


Fig. 2 Cross-sectional distributions of RBCs and drug carriers for generalized plasma skimming model. α is the relative distribution between RBCs and drug carriers. At $\alpha = 0$, all drug carriers remain in the RBC core. When α is increased, drug carrier distribution shifts toward CFL.

vessels, respectively. If two daughter vessels have the same vessel diameter, ζ^b values for determining hematocrit of daughter vessels are also identical such that the hematocrit values of daughter vessels are the same with that of parent vessel. In most cases, however, two daughter vessels have different diameters. If the diameters of two daughter vessels greatly differ, the thicker daughter vessel has higher ζ^b and the thinner daughter vessel has lower ζ^b . Note that while ζ^b is a dimensionless kinematic quantity relating the relative phase velocities in terms of the ratio of parent to daughter vessel cross-sectional areas, the absolute number of ζ^b does not describe plasma skimming. Only the relative difference between ζ^b of the daughter vessels affects the hematocrit of daughter vessels. Whilst there are other mathematically simple and validated plasma skimming models (Pries and Secomb 2005; Guibert et al. 2010), the model developed by Gould et al. (Gould and Linninger 2015) was considered due to its easy extensibility.

2.2 Generalized plasma skimming model for cells and drug carriers

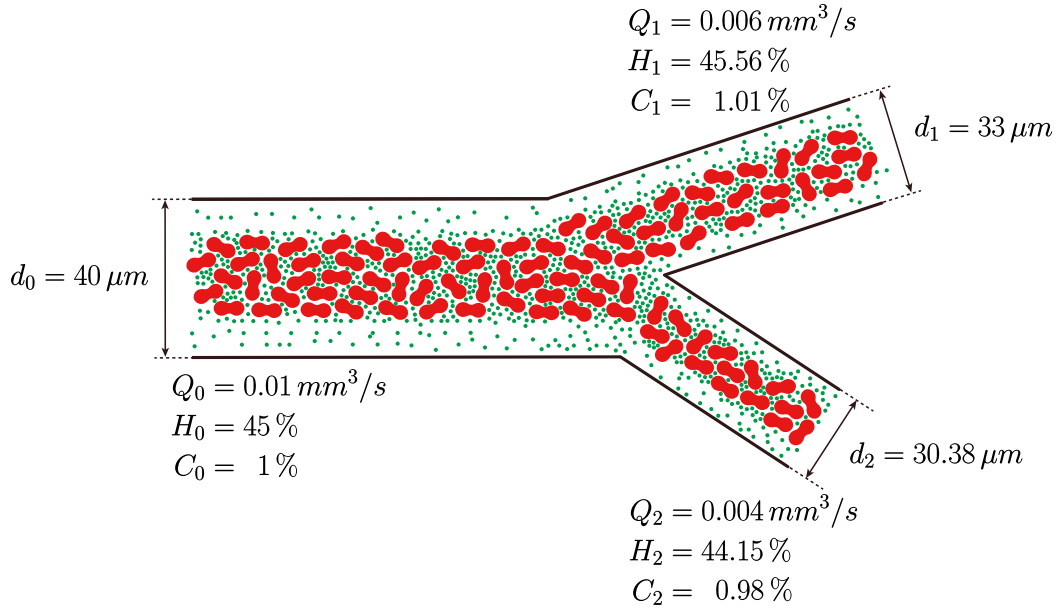
The changes in hematocrit due to the plasma skimming are a special case of mass transport at a bifurcation. In order to mathematically model the distribution of drug carriers or any cells, which may not necessarily be the same as the one of RBCs, a generalized plasma skimming model was constructed by adding a distribution-shape parameter α to the plasma skimming model of blood (Gould and Linninger 2015) as follows:

$$C_1 = C_0 - \Delta C = \zeta_1^c C^* \quad (5)$$

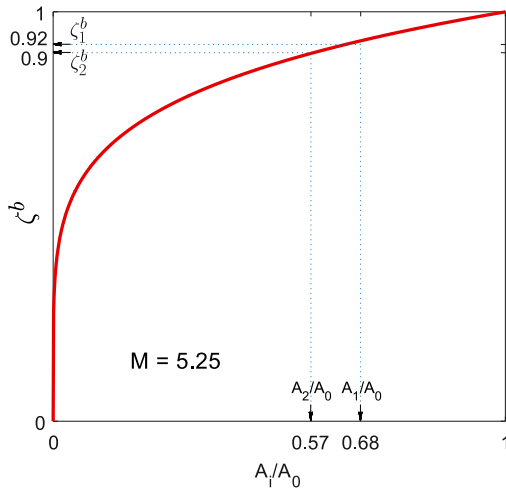
$$C_2 = \zeta_2^c C^* \quad (6)$$

$$Q_0 C_0 = Q_1 C_1 + Q_2 C_2 = Q_1 \zeta_1^c C^* + Q_2 \zeta_2^c C^* \quad (7)$$

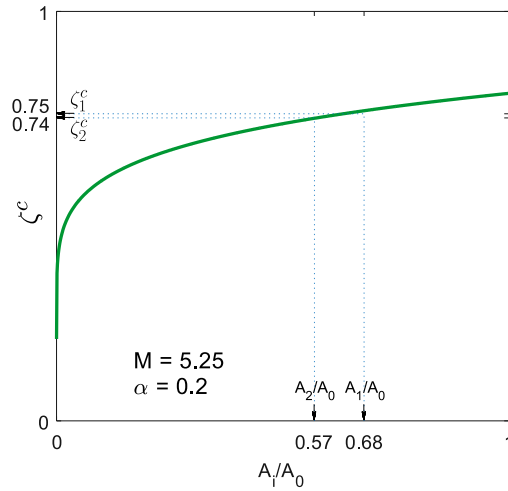
$$\zeta_i^c = (1-\alpha) \left(\frac{A_i}{A_0} \right)^{\frac{1}{M}} + \alpha \left\{ 1 - \left(\frac{A_i}{A_0} \right)^{\frac{1}{M}} \right\} \quad \text{where } i = 1, 2$$



(a) Redistributions of RBCs and drug carriers at a bifurcation



(b) Hematocrit distribution at bifurcations



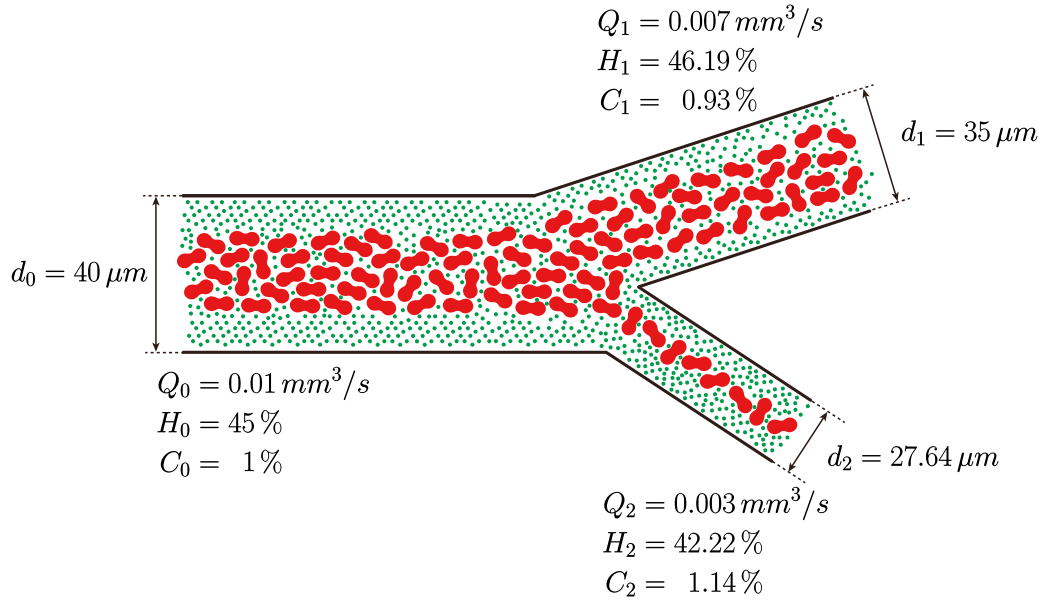
(c) Drug carrier distribution at bifurcations

Fig. 3 Redistribution of RBCs and drug carriers with $\alpha = 0.2$ at a bifurcation. Low α indicates drug carriers stay in the RBC core of parent microvessel. After the bifurcating process, RBCs and drug carriers are redistributed in the daughter vessels. (a) Schematic diagram of single bifurcation with RBCs and drug carriers. (b) ζ^b curve for calculating hematocrit in daughter microvessels. (c) ζ^c curve for calculating concentration of drug carriers in daughter microvessels.

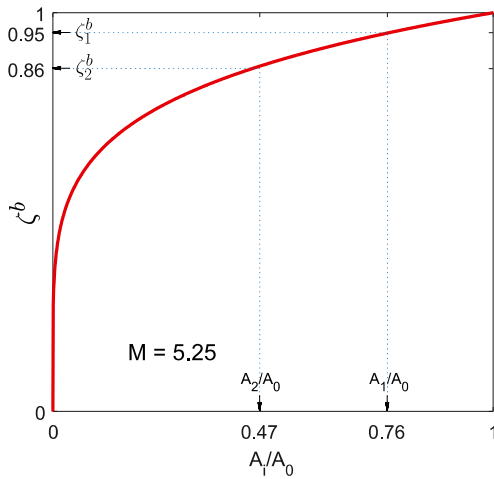
(8)

where C is the concentration of cells or drug carriers, ζ^c is the concentration change coefficient and α is the shape parameter for cross-sectional distribution of C in a microvessel, as described in Fig. 2. In the case of $\alpha = 0$, all cells or drug carriers are within RBC region, equivalent to the original plasma skimming model for RBCs. On the other hand, when $\alpha = 1$, all cells or drug carriers are within CFL region. They are redistributed by the opposite tendency of plasma skimming. In most cases α is likely to be somewhere between 0 and 1. For

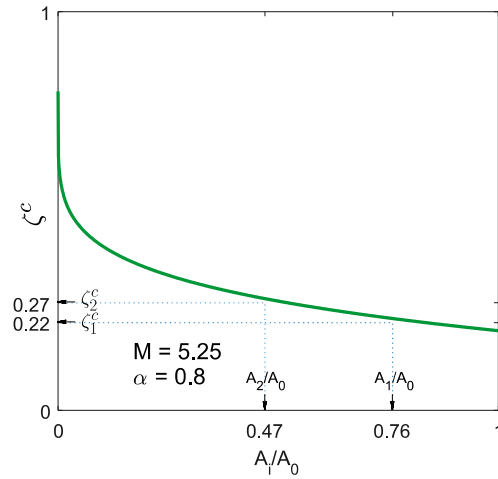
example, in a previous work (Lee et al. 2013), it was reported that larger particles stay in CFL region and smaller particles stay in RBC core. In this case, particle size is proportional to α . Therefore, in such case, α effectively becomes an indicator to quantify the transport efficiency in capillary beds. In order to simplify the model, cells or drug carriers were assumed to be homogeneous in both RBC and CFL regions with α representing the relative level of cells or drug carriers in the two regions. The shape parameter α enables the modeling of drug carrier redistribution after bifurcation tailored to the characteristics of specific drug carriers,



(a) Redistributions of RBCs and drug carriers at a bifurcation



(b) Hematocrit distribution at bifurcations



(c) Drug carrier distribution at bifurcations

Fig. 4 Redistribution of RBCs and drug carriers with $\alpha = 0.8$ at a bifurcation. High α indicates drug carriers stay in the CFL area of parent microvessel. After the bifurcating process, RBCs and drug carriers are redistributed in the daughter vessels. (a) Schematic diagram of single bifurcation with RBCs and drug carriers. (b) ζ^b curve for calculating hematocrit in daughter microvessels. (c) ζ^c curve for calculating concentration of drug carriers in daughter microvessels.

and hence making the model to be very generalized. Therefore, if α of a specific drug carrier is studied, this mathematical model can be adjusted on it.

2.3 Coupling the generalized plasma skimming model with blood flow in the microvasculature

Computing drug carrier distribution by using the generalized plasma skimming model is simple in a single bifurcation case. However, it is challenging to predict distributions of cells and drug carriers in the en-

tire microvascular network. If one is to consider individual RBCs and drug carriers in a microvascular network with thousands of vessel segments, it requires tremendous amount of computation time with heavy parallel processing. Furthermore, *in vivo* experiments are still challenging to accurately measure the distributions. In order to greatly reduce the computation time while obtaining feasible solutions, the generalized plasma skimming model was coupled with the mathematical model of blood flow to predict the distributions. The microvascular network geometry was computationally generated based on mathematical algorithms,

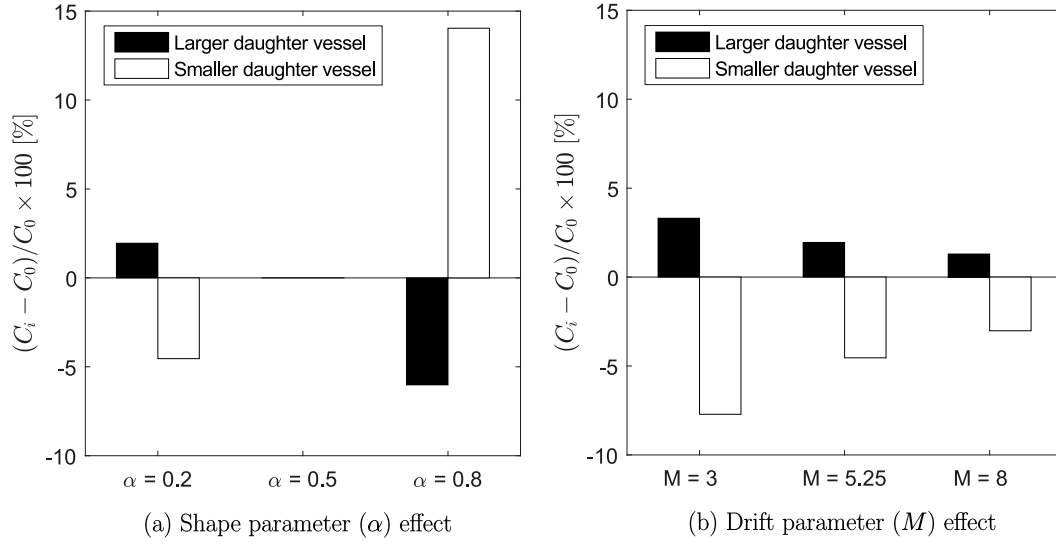


Fig. 5 Effects of α and M in a single bifurcation model. The average changes in drug carrier distribution were calculated for a single bifurcation model with different α and M . (a) Three α values were tested. When $\alpha = 0.5$, drug carriers in the parent vessel were uniformly distributed throughout the vessel's cross-section, hence not producing any change in drug carrier redistribution. With $\alpha < 0.5$, since drug carriers are highly accumulated in the RBC core, the concentration of drug carriers in the larger daughter vessel was increased. On the other hand, for $\alpha > 0.5$, the concentration of drug carriers in the smaller daughter vessel was increased up to 14 %. (b) When $\alpha = 0.2$, the drift parameter, M , effect was investigated by applying three M values. When M is low, the concentration of drug carriers in the daughter vessels was significantly changed.

not from scanned images, by choosing vessel diameter (d_i), vessel length (l_i) and bifurcation angles (θ_i and ϕ_i) (Yang et al. 2016). Three diameters for each bifurcation (one parent vessel and two daughter vessels) were governed by $d_0^\gamma = d_1^\gamma + d_2^\gamma$ where γ was fixed at 3 (Sherman 1981; Murray 1926). For defining the vessels' lengths from their diameters, the length-to-diameter ratio ($\beta = l/d$) was fixed at 25 (Yang et al. 2016). Flow rates of blood (Q_i) were calculated by Poiseuille's law and the *in vivo* viscosity (Pries et al. 1996):

$$Q_i = \frac{\pi d_i^4}{128 \mu_i l_i} \Delta P_i \quad (9)$$

$$\mu_i = \mu_p \left[1 + (\mu_{0.45}^* - 1) \frac{(1 - H_D)^C - 1}{(1 - 0.45)^C - 1} \times \left(\frac{d}{d - 1.1} \right)^2 \right] \left(\frac{d}{d - 1.1} \right)^2 \quad (10)$$

$$\mu_{0.45}^* = 6e^{-0.085d} + 3.2 - 2.44e^{-0.06d^{0.645}} \quad (11)$$

$$C = (0.8 + e^{-0.075d}) \left(-1 + \frac{1}{1 + 10^{-11}d^{12}} \right) + \frac{1}{1 + 10^{-11}d^{12}}. \quad (12)$$

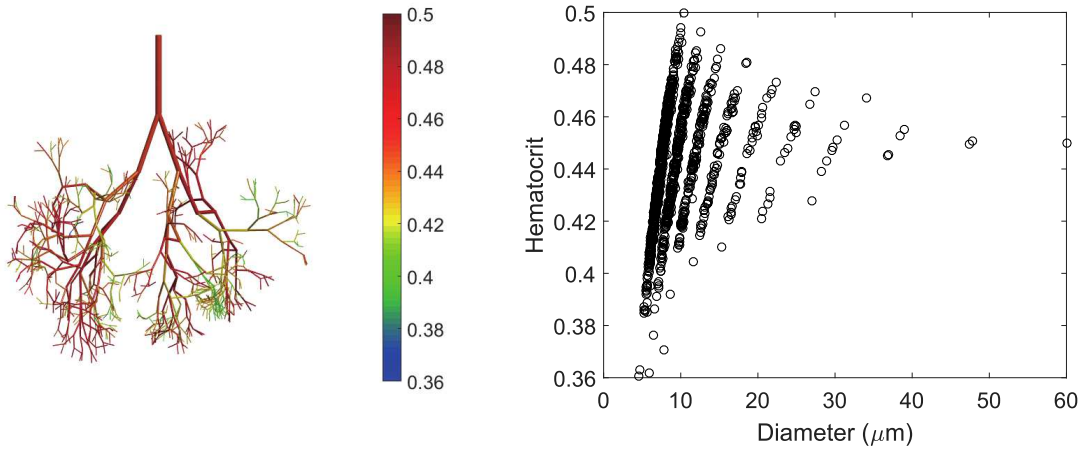
Here, μ_i is the apparent viscosity of blood and μ_p is the reference viscosity of plasma, fixed at $9 \cdot 10^{-6}$ mmHg·s (Yang and Wang 2013). H_D is the discharge hematocrit, which was calculated by Eqs. (1), (2), (3) and

(4). Also, three flow rates at each bifurcation were calculated by conservation of mass, $\sum Q_i = 0$. By assuming that the microvascular transport of drug carriers is independent of the blood flow, the drug carrier distribution can be calculated by explicitly coupling blood flow rates in microvessels with the generalized plasma skimming model. Note that the drift parameter, M , is identical with that for hematocrit calculation, and the proposed model is fully coupled with hematocrit and plasma skimming of RBCs.

3 Results

3.1 Plasma skimming of drug carriers in a single bifurcation model

The single bifurcation model used for testing the plasma skimming effects is given in Fig. 3a. The diameters of a parent and two daughter vessels were 40, 33 and 30.38 μm , respectively. The flow rates of three microvessels were 0.01, 0.006 and 0.004 mm^3/s , respectively. In the parent vessel, the hematocrit (H_0) and the concentration of drug carriers (C_0) were given as 45 % and 1 % of whole blood volume. In microvascular transport, the concentration of RBCs is increased in the larger daughter vessel and decreased in the smaller daughter vessel due to the plasma skimming effect. The hematocrit changes in two daughter vessels were calculated by Eqs. (1)-(4). The drift parameter, M for *in vivo* microvas-



(a) Hematocrit distribution

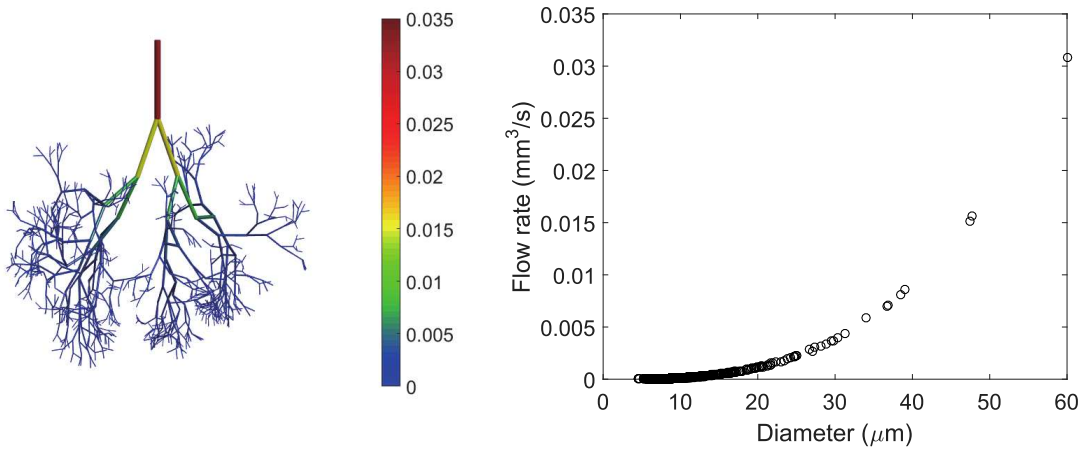
(b) Flow rate (mm^3/s)

Fig. 6 Representative model of microvascular transport in a microvascular network. The microvasculature geometry was constructed by a computational algorithm with model parameters, $\gamma = 3$ and $\beta = 25$ with root vessel diameter = $60 \mu m$. The pressure drops between the root vessel and the capillary ends were 60 mmHg. (a) Hematocrit distribution along diameter. The hematocrit distribution was calculated by Gould and Linninger (2015)'s method. (b) Flow rates along diameter. The blood flow in the microvessels was calculated by Poiseuille's law with the *in vivo* viscosity law (Pries et al. 1996).

cular network was fixed at 5.25 as previously reported (Gould and Linninger 2015).

From the given conditions, hematocrit changes followed the curve in Fig. 3b. The hematocrit in larger daughter vessel was increased to 45.56 % and the hematocrit in smaller daughter vessel was decreased to 44.15 %. In a single bifurcation model, the concentration changes in drug carriers in two daughter vessels are predicted by Eqs. (5)-(8). As shown in Fig. 2, drug carriers are concentrated on the RBC core at $\alpha = 0.2$. Therefore, the concentration changes in drug carriers should follow the same trend of blood hematocrit. The concentration in the larger daughter vessel, C_1 was 1.01% (increased) and the concentration in the smaller daughter vessel, C_2 was 0.98 % (decreased) (Fig. 3c), hence showing the expected tendency.

Figure 4a shows the redistribution of RBCs and drug carriers at $\alpha = 0.8$. Initial concentration of drug carriers was low in RBC core and high in CFL, which means drug carriers tend to easily escape from RBC core and marginate toward CFL. Then, the plasma skimming at the bifurcation caused drug carriers to accumulate in the smaller daughter vessel, or in better words, in the vessel where there is more CFL. Consequently, the concentration of drug carriers was decreased in larger daughter vessel and increased in smaller daughter vessel. The hematocrit changes, ζ_b , are proportional to the diameter changes, A_i/A_0 , as plotted in Fig. 4b. On the other hand, the concentration changes in drug carriers, ζ^c , are inversely proportional to A_i/A_0 , as described in Fig. 4c. The concentration of drug carriers in the larger daughter vessel, C_1 , was decreased to 0.93 % compared

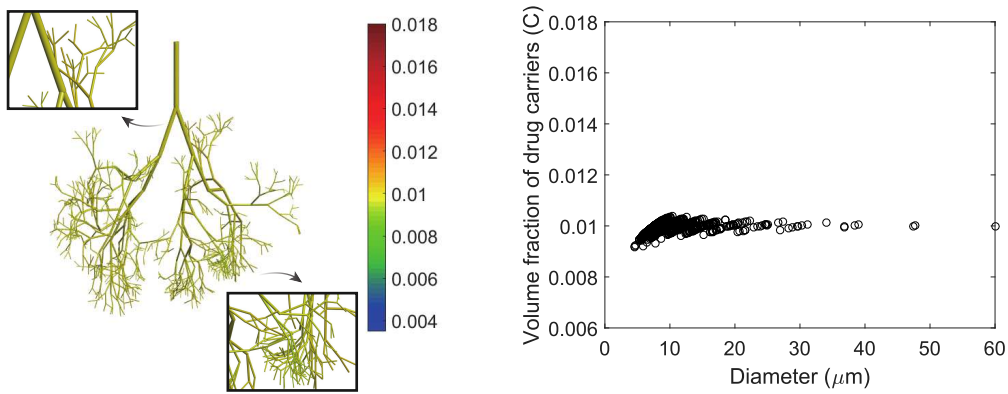
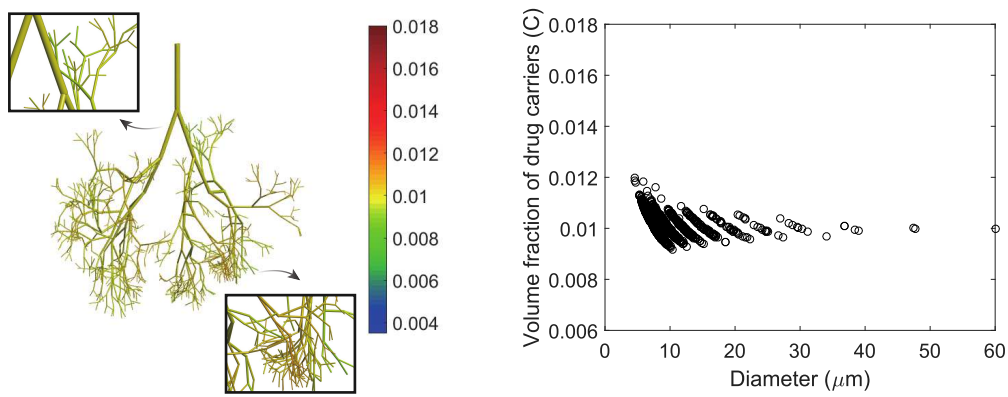
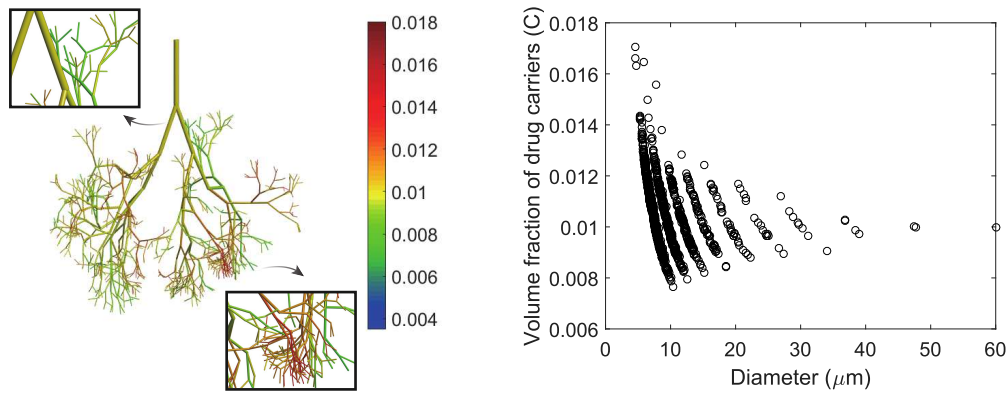
(a) Volume fraction of drug carriers ($\alpha = 0.2$)(b) Volume fraction of drug carriers ($\alpha = 0.5$)(c) Volume fraction of drug carriers ($\alpha = 0.8$)

Fig. 7 Redistribution of drug carriers in the microvasculature. The drug carrier distribution was calculated by Eqs. (5)-(8). Three α values were used to predict the redistribution tendency of drug carriers in the computational microvasculature model. The initial concentration of drug carriers in the root vessel was 0.01. By increasing α , the concentration of drug carriers in the capillary beds, below $10 \mu\text{m}$ diameters, was in the range from 0.008 to 0.017, and the average concentration in the capillary beds was increased.

to $C_0 = 1\%$. Moreover, the concentration of drug carriers in the smaller daughter vessel, C_2 , was increased to 1.14 %.

The effect of shape parameter on drug carrier redistribution is summarized in Fig. 5a. The initial and boundary conditions of single bifurcation were the same with that in Fig. 4a. Note that the concentration changes at $\alpha = 0.5$ were zeros for both daughter vessels because the drug carriers were uniformly distributed in the microvessel. At $\alpha = 0.2$, the concentration of drug carriers was increased by 2 % in the larger daughter vessel and decreased by 5 % in the smaller daughter vessel. On the other hand, at $\alpha = 0.8$, the concentration of drug carriers was decreased by 7 % in the larger daughter vessel and increased by 14 % in the smaller daughter vessel. In Fig. 5b, the effect of drift parameter, M , is investigated at $\alpha = 0.2$. High M implies well-mixed RBCs and plasma. Low M implies highly separated RBC core and CFL. The model was tested with three cases at $M = 3, 5.25$ and 8 , and the concentration changes in drug carriers showed increasing tendency for decreasing M . Intuitively, at $M = 3$ or lower, separated RBC core and CFL regions change the distribution of drug carriers. At $M = 8$, the well-mixed blood makes the distribution of drug carriers to stabilize.

3.2 Generalized plasma skimming of drug carriers in the microvasculature

The generalized plasma skimming model for RBCs and drug carriers was applied to predict their distributions in the microvascular network. The mathematically generated computational microvasculature model mentioned in Section 2.3 was used. Note that this computational microvasculature model is limited for generating binary tree-like structures. However, *in vivo* capillary beds form loops, anastomoses, and multifurcations. Therefore, for a more realistic analysis it is necessary to consider a true network of microvessels rather than just continuously bifurcating microvessels. Despite such limitation, this binary tree-like structure is sufficient for studying drug carrier redistribution in continuously branching microvessels. For generating a more realistic microvascular network, one can refer to the computational microvasculature constructed by Linninger et al. (2013). From the root vessel with $60\ \mu\text{m}$ diameter, the vessel segment was bifurcated ten times until the diameters were decreased to under $10\ \mu\text{m}$, with $\beta = 25$ (Yang et al. 2016). The boundary condition was $60\ \text{mmHg}$ pressure drops between inlet root vessel and outlet capillary ends. For calculating hematocrit distributions, the drift parameter, M , was fixed at 5.25 (Gould and Linninger 2015). The initial hematocrit in the root vessel was

0.45 . Figure 6 shows the hematocrit distributions and flow rates in the given microvascular network. Unlike the initial hematocrit in the root vessel, the hematocrit distribution was significantly changed due to plasma skimming. In capillary ends, blood hematocrit was in the range from 0.35 to 0.5 . Based on the hematocrit and *in vivo* viscosity law, flow rates of blood were calculated and plotted along with diameter in Fig. 6b. Furthermore, the volumetric flow rate was proportional to vessel diameter, as plotted in Fig. 6b.

In the microvascular transport of blood in the microvasculature, the distribution of drug carriers was predicted by Eqs. (5)-(8). The initial volume fraction of drug carrier was 0.01 . Three cross-sectional distributions of drug carriers, $\alpha = 0.2, 0.5$ and 0.8 , were applied to the computational microvasculature model. Figure 7 shows the results at $\alpha = 0.2, 0.5$ and 0.8 . When α was higher, the drug carriers were accumulated in the capillary beds with high variances, ranging from 0.008 to 0.017 . From these results, it is expected that highly accumulated drug carriers in CFL of large root vessels can move to capillary ends quickly by following the plasma skimming of blood. For quantitatively evaluating the average accumulation of drug carriers in the capillary ends, an average volume fraction is defined as:

$$\bar{C} = \frac{1}{n_{cap}} \sum_{i=1}^{n_{cap}} C_i \quad (13)$$

where \bar{C} is the average volume fraction of drug carriers and n_{cap} is the total number of microvessels with diameters below $10\ \mu\text{m}$. The relative variance of volume fraction is $(\bar{C} - C_0)/C_0 \times 100\%$ where C_0 is the initial volume fraction of drug carriers. Note that $C_0 = 0.01$ (or 1%). Figure 8 shows the changes in average volume fraction for the α range from 0.2 to 0.8 . Interestingly, when α was increased, the average accumulation of drug carriers in capillary ends was quasi-linearly increased up to 10% of initial volume fraction. Figure 9 shows the redistribution of drug carriers in the microvascular network with respect to hematocrit and diameter. At $\alpha = 0.2$, the volume fraction of drug carriers was slightly changed. However, as plotted in Fig. 9c, in the case of low hematocrit and small diameter vessel at $\alpha = 0.8$, the volume fraction of drug carriers was greatly increased.

4 Discussion

The generalized plasma skimming model was developed for predicting the distributions of cells and drug carriers in the microvasculature. As expected, the concentration of drug carriers in the microvasculature was highly

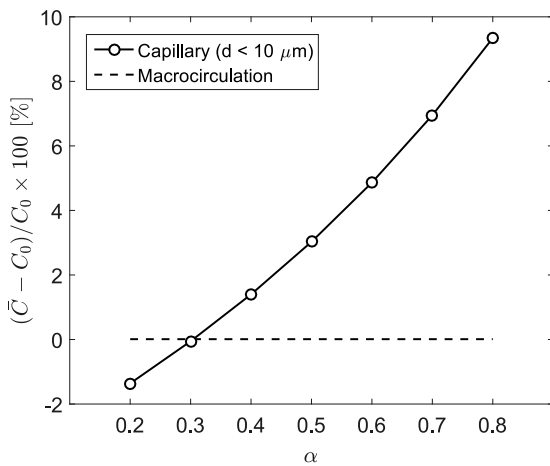


Fig. 8 Effect of α in a microvascular system. The average concentration of drug carriers with different α values was predicted in the microvascular system. The initial concentration of drug carriers in the root vessel was assumed to be the same as the one in the macrocirculation.

changed by the plasma skimming of blood. Firstly, in a single bifurcation, the redistributions of RBCs and drug carriers were calculated at two α values, which represent RBC core concentrated drug carriers ($\alpha = 0.2$) and CFL concentrated drug carriers ($\alpha = 0.8$). Secondly, the generalized plasma skimming model was applied to predict the concentration of drug carriers in the microvasculature. Furthermore, the redistribution of drug carriers was correlated with hematocrit and their cross-sectional distribution in the entire microvasculature. Therefore, if the specific parameters of microvascular environment are given for targeting diseased areas, the design of drug carriers can be suggested by this mathematical model, specifically by selecting cross-sectional distribution of drug carriers, called shape parameter, α .

Related to this topic, Thomas et al. (2014) fully discussed about the effect of vessel bifurcation in delivering nanoparticles with different sizes. From the experiments, it was found that the drug delivering efficiency was highly related to the microvascular environment. However, it is still challenging to quantitatively measure the concentration of drug carriers *in vivo* mouse models. Also, due to the limited information from experiments, it is difficult to decide the design of drug carriers for targeting specific microvascular environments. Hence, the mathematical model of blood flow coupled with the generalized plasma skimming model can be used as a predictive tool that can estimate the delivering efficiency of drug carriers. For the prediction, the shape parameter, α , can be the indicator for predicting whether the drug carriers are fast accumulated in the capillary beds. For example, as plotted in Fig. 8, when α is below 0.3, the concentration of drug carriers was

lower than the concentration in the macrocirculation. Therefore, it is possible to give a guideline to enhance the accumulation in the capillary beds by applying α of drug carriers. In the current analysis, $\alpha = 0.3$ was considered.

It must be noted that the plasma skimming model developed by Gould et al. is capable of addressing multifurcations. The proposed method in this study is a simple extension of the drift flux model. Hence, whilst this study used a binary tree-like structure for studying drug carrier redistribution, this new model is also perfectly applicable to multifurcating microvasculature. Furthermore, by no means this study aims to provide the drug carrier specific value of shape parameter α and its physical interpretation. Its interpretation described in Section 3.2 is only an example of how the drug carriers are likely to be redistributed. Such interpretation is based on the idea that if drug carriers have good margination, they are likely to move with plasma after bifurcation, not RBCs in the core, and vice-versa. This shape parameter α makes the proposed model to be very generalized. By adjusting only a single parameter, the mathematical model can be easily tailored to a specific drug carrier redistribution problem.

For the correlation between α and targeting efficiency, various parametric studies *in silico*, *in vitro* and *in vivo* will be required. However, this study was aimed at developing a mathematical model. To correlate the current model to a real system, the parameters for the generalized plasma skimming model must be obtained from *in vitro* and *in vivo* experiments. Also, the correlation between M and α needs to be further investigated by conducting detailed numerical simulations with individual RBCs, drug carriers, and blood plasma. By overcoming all these limitations, it is hoped to utilize this new model for precisely targeting diseased areas in microvascular networks.

Acknowledgment

This research was supported by Basic Science Research Program through the National Research Foundation of Korea (KRF) funded by the Ministry of Education (NRF-2015R1D1A1A01060992), and by the Bio & Medical Technology Development Program of the National Research Foundation (NRF) funded by the Ministry of Science, ICT & Future Planning (2016M3A9B4919711).

Conflict of Interest

The authors declare that they have no conflict of interest.

References

- Champion JA, Walker A, Mitragotri S (2008) Role of particle size in phagocytosis of polymeric microspheres. *Pharmaceutical research* 25(8):1815–1821
- Chauhan VP, Stylianopoulos T, Martin JD, Popović Z, Chen O, Kamoun WS, Bawendi MG, Fukumura D, Jain RK (2012) Normalization of tumour blood vessels improves the delivery of nanomedicines in a size-dependent manner. *Nature nanotechnology* 7(6):383–388
- Curtis LT, Wu M, Lowengrub J, Decuzzi P, Frieboes HB (2015) Computational modeling of tumor response to drug release from vasculature-bound nanoparticles. *PloS one* 10(12):e0144,888
- D’Apolito R, Taraballi F, Minardi S, Liu X, Caserta S, Cevenini A, Tasciotti E, Tomaiuolo G, Guido S (2016) Microfluidic interactions between red blood cells and drug carriers by image analysis techniques. *Medical engineering & physics* 38(1):17–23
- Frieboes HB, Wu M, Lowengrub J, Decuzzi P, Cristini V (2013) A computational model for predicting nanoparticle accumulation in tumor vasculature. *PloS one* 8(2):e56,876
- Gould IG, Linninger AA (2015) Hematocrit distribution and tissue oxygenation in large microcirculatory networks. *Microcirculation* 22(1):1–18
- Guibert R, Fonta C, Plouraboué F (2010) A new approach to model confined suspensions flows in complex networks: application to blood flow. *Transport in porous media* 83(1):171–194
- Jain RK, Stylianopoulos T (2010) Delivering nanomedicine to solid tumors. *Nature reviews Clinical oncology* 7(11):653–664
- Kamoun WS, Chae SS, Lacorre DA, Tyrrell JA, Mitre M, Gillissen MA, Fukumura D, Jain RK, Munn LL (2010) Simultaneous measurement of rbc velocity, flux, hematocrit and shear rate in vascular networks. *Nature methods* 7(8):655–660
- Krogh A, Harrop G, Rehberg PB (1922) Studies on the physiology of capillaries: iii. the innervation of the blood vessels in the hind legs of the frog. *The Journal of physiology* 56(3-4):179
- Lee TR, Choi M, Kopacz AM, Yun SH, Liu WK, Decuzzi P (2013) On the near-wall accumulation of injectable particles in the microcirculation: smaller is not better. *Scientific reports* 3
- Lee TR, Greene MS, Jiang Z, Kopacz AM, Decuzzi P, Chen W, Liu WK (2014) Quantifying uncertainties in the microvascular transport of nanoparticles. *Biomechanics and modeling in mechanobiology* 13(3):515–526
- Linninger AA, Gould I, Marinnan T, Hsu CY, Chojecki M, Alaraj A (2013) Cerebral microcirculation and oxygen tension in the human secondary cortex. *Annals of biomedical engineering* 41(11):2264–2284
- Müller K, Fedosov DA, Gompper G (2014) Margination of micro-and nano-particles in blood flow and its effect on drug delivery. *Scientific reports* 4
- Muro S, Garnacho C, Champion JA, Leferovich J, Gajewski C, Schuchman EH, Mitragotri S, Muzykantov VR (2008) Control of endothelial targeting and intracellular delivery of therapeutic enzymes by modulating the size and shape of icam-1-targeted carriers. *Molecular Therapy* 16(8):1450–1458
- Murray CD (1926) The physiological principle of minimum work applied to the angle of branching of arteries. *J Gen Physiol* 9:835–841
- Namdee K, Thompson AJ, Golinski A, Mocherla S, Bouis D, Eniola-Adefeso O (2014) In vivo evaluation of vascular-targeted spheroidal microparticles for imaging and drug delivery application in atherosclerosis. *Atherosclerosis* 237(1):279–286
- Peer D, Karp JM, Hong S, Farokhzad OC, Margalit R, Langer R (2007) Nanocarriers as an emerging platform for cancer therapy. *Nature nanotechnology* 2(12):751–760
- Pries AR, Secomb TW (2005) Microvascular blood viscosity in vivo and the endothelial surface layer. *American Journal of Physiology-Heart and Circulatory Physiology* 289(6):H2657–H2664
- Pries AR, Secomb TW, Gaehtgens P (1996) Biophysical aspects of blood flow in the microvasculature. *Cardiovascular Research* 32:654–667
- Saadatmand M, Ishikawa T, Matsuki N, Abdekhodaie MJ, Imai Y, Ueno H, Yamaguchi T (2011) Fluid particle diffusion through high-hematocrit blood flow within a capillary tube. *Journal of biomechanics* 44(1):170–175
- Sherman TF (1981) On connecting large vessels to small. the meaning of murray’s law. *The Journal of general physiology* 78(4):431–453
- Sobczynski DJ, Fish MB, Fromen CA, Carasco-Teja M, Coleman RM, Eniola-Adefeso O (2015) Drug carrier interaction with blood: a critical aspect for high-efficient vascular-targeted drug delivery systems. *Therapeutic delivery* 6(8):915–934
- Tan J, Shah S, Thomas A, Ou-Yang HD, Liu Y (2013) The influence of size, shape and vessel geometry on nanoparticle distribution. *Microfluidics and nanofluidics* 14(1-2):77–87
- Tan J, Keller W, Sohrabi S, Yang J, Liu Y (2016) Characterization of nanoparticle dispersion in red blood cell suspension by the lattice boltzmann-immersed boundary method. *Nanomaterials* 6(2):30

- Thomas A, Tan J, Liu Y (2014) Characterization of nanoparticle delivery in microcirculation using a microfluidic device. *Microvascular research* 94:17–27
- van de Ven AL, Kim P, Fakhoury JR, Adriani G, Schmulen J, Moloney P, Hussain F, Ferrari M, Liu X, Yun SH, et al. (2012) Rapid tumortropic accumulation of systemically injected plateloid particles and their biodistribution. *Journal of Controlled Release* 158(1):148–155
- Yang J, Wang Y (2013) Design of vascular networks : A mathematical model approach. *International journal for numerical methods in biomedical engineering* 29(4):515–529
- Yang J, Pak YE, Lee TR (2016) Predicting bifurcation angle effect on blood flow in the microvasculature. *Microvascular Research* 108:22–28

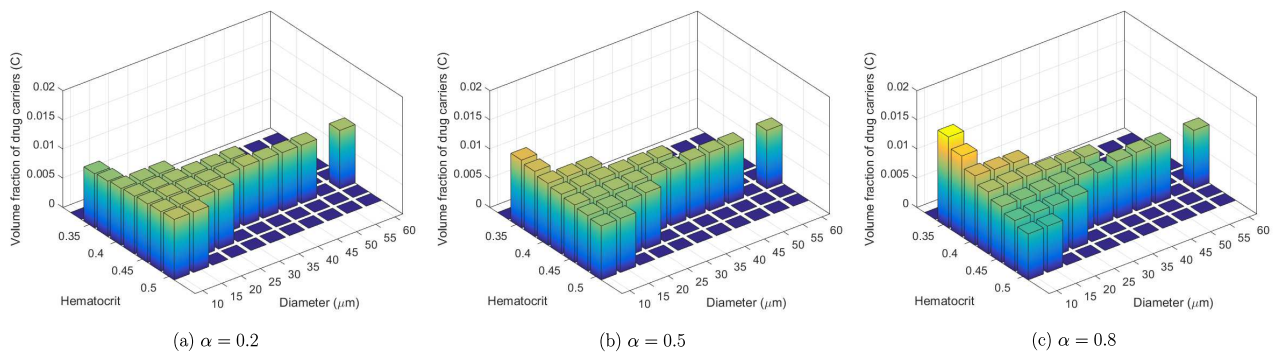


Fig. 9 Effect of α along with vessel diameter and hematocrit in a microvascular system. The concentration of drug carriers are plotted along with hematocrit and vessel diameter. Three α cases were tested in the computational microvascular network model.